Dental X-Ray: A Data Set of Panoramic Dental Radiographs for Stomatologic Image Processing Purposes

João Oliveira & Hugo Proença
Department of Computer Science of University of Beira Interior, Covilhã, Portugal

This paper has two major purposes: at firstly, to announce the availability of a new data set of panoramic dental X-ray images. This data set contains 1392 images with varying types of noise, usually inherent to this kind of images. Furthermore, the number of teeth per image and their dental morphology were not constant. Secondly, we propose a method to approximate the panoramic images in bitewing images, which are the most common type of images used in the human identification and in the tooth segmentation for the diagnosis of dental diseases.
Keywords: Dental X-ray; Data Set; Medical Image; Image Processing; Computer Vision;

1   INTRODUCTION

Automated image analysis processes have been achieving higher relevance for many purposes and the results can be considered satisfactory (*e.g.*, biometrics and multiple types of medical image diagnosis). In the specific area of medical image processing these automated systems constitute a valuable tool as the earliest detection of many diseases and in the preprocessing of huge amounts of data.

This paper announces the availability for research purposes of a new data set of panoramic dental radiograph images. Nowadays, there are a variety of areas where this type of images can be helpful: biometrics identification (Jain, Chen, and Minut 2003)(Jain, Hong, and Pankanti 2000)(Chen and Jain 2004) (Jain and Chen 2004) (Nomir and Abdel-Mottaleb 2005) (Zhou and Abdel-Mottaleb 2005) (Nomir and Abdel-Mottaleb 2007) (Nomir and Abdel-Mottaleb 2008), detection of dental cavities, bone loss and periodontitis (Li, Fevens, Krzyzak, and Li 2006) (Li, Fevens, Krzyzak, Jin, and Li 2007) (Shiffman, Rubin, and Naple 2000). However, the types of images that are usually chosen for these purposes are the bitewing and the periapical, used to perform the tooth segmentation (Shah, Abaza, Ross, and Ammar 2006) (Said, Nassar, Fahmy, and Ammar 2006) (Lin, Cheng, and Mao 1996) and to identify deceased individuals (Chen and Jain 2004) (Jain and Chen 2004) (Nomir and Abdel-Mottaleb 2005) (Zhou and Abdel-Mottaleb 2005) (Shah, Abaza, Ross, and Ammar 2006) (Said, Nassar, Fahmy, and Ammar 2006) (Nomir and Abdel-

Mottaleb 2008). Here, having access to the AM (*ante-mortem*) and PM (*post-mortem*) dental X-ray, is in some cases the only way to identify such individuals. Finally, these types of images are also used in clinical environments,in the detection of dental diseases (Li, Fevens, Krzyzak, and Li 2006) (Li, Fevens, Krzyzak, Jin, and Li 2007).

According to the above discussion, in this paper we also propose a method that approximate the panoramic dental X-ray images into bitewing dental X-ray images used by many authors. This method comprises three stages, the first stage is based on a statistical evaluation of the images to define a preliminary region-of-interest (ROI), taking out the nasal and chin bones. In the second stage we make the detection of the upper and lower jaws, based on the extraction of primitive points between jaws and a polynomial fitting process. The third stage is the partition of each jaw into three parts. The left side contains the left molars and the left pre-molars, the front side includes the canines and the incisors and, finally, the right side that contains the right molars and the right pre-molars.

Another major point of interest of this data set is the set of maps that enable the manual detection and localization of dental cavities - for the moment - and other diseases in a near future. This is achieved by corresponding a binary image to each dental X-ray image thereby showing the regions with dental cavities. This will turn the data set into a preferable tool in the evaluation of method to perform automatic detection and localization of the respective diseases.

Also, we believe that this set of images is useful to evaluate the current teeth segmentation methods.

The remaining of this paper is organized as follows. In Section 2 we present the most relevant features of the data set. Section 3 describes the proposed method to transform the panoramic dental X-ray images into bitewing images. Section 4 reports our experiments and, finally, Section 5 gives the conclusions and future work.

2 Data Set

In this sub-section we describe the main points of the data set images wich were all captured by an Orthoralix 9200 DDE X-ray camera. There are a total of 1392 grayscale images in the data set, with varying types of dental structure, sizes of the mouth and number of teeth per image, as can be seen in figure 1. The gray levels of each image were stretched to the [0, 255] scale, although both normalized and raw images will be soon available for download in the site SociaLab[1]
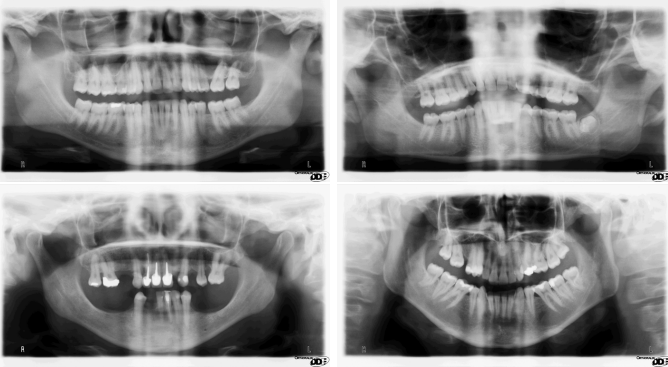

Figure 1: Examples of images of the Dental X-ray data set.

When compared with other types of stomatology images, radiographic images are highly challenging, due to several reasons that increase their heterogeneity. Firstly, different levels of noise, due to the moving imaging device that captures a global perspective of the patient's mouth. Secondly, low contrast, either global or on local regions of the images, the topology and morphologic properties are very complex. Thirdly the blurring that denies the straightforward detection of edges and finally the spinal-column that covers the frontal teeth in some images, as shown in figure 1.

We considered that images contains all teeth in two different circumstances, first when the images include only the first and second molar, superior or inferior and left or right along with all other teeth. Second is when the images contain all three molars superior or

---

inferior and left or right in addition to all other teeth. In order to more effectively use the images we named them according to their characteristics. With this arrangement we classify the images based on the number of teeth and in the existence of dental cavities. The naming takes the form *It1_t2_t3.tiff*, where *t1* corresponds to the image number, *t2* represents the quantity of teeth per mouth (0 refers to no teeth, 1 to some teeth and 2 to all teeth) and *t3* denominates the presence of dental cavities in the image (0 corresponds to no dental cavities and 1 to the presence of dental cavities). As an example, the name *I1200_2_0.tiff* corresponds to the image with id equal to 1200, which has all teeth and no dental cavities.

3 Proposed Method to Approximate Panoramic images Into Bitewing images

In this section we detail the proposed method to transform the original images into bitewing images. It consists in three different stages, as shown in the block diagram of figure 2:
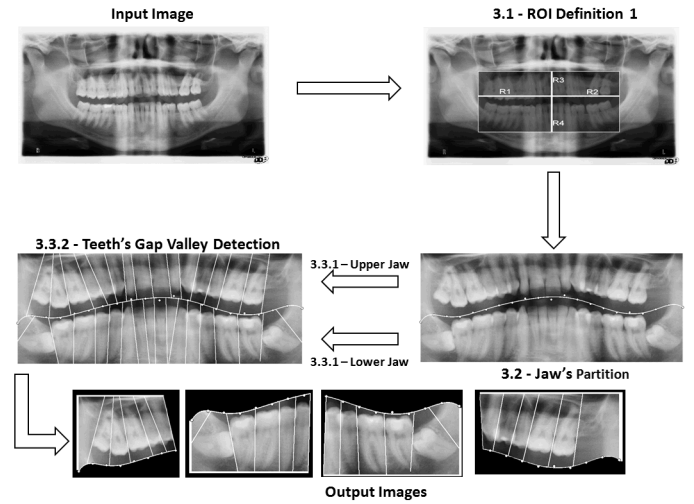

Figure 2: Block Diagram of the proposed method.

3.1 Statistical Analysis

The earliest stage is based in the statistical analysis of the sizes and positions of each component in each image, in order to define an initial region of interest. This eliminates non-useful information originated by the nasal and chin bones. Our purpose is to crop a region that contains the entire mouth and eliminate the maximum amount of noise possible. For each data set image we measured four distances (R_1, R_2, R_3, R_4), starting from the image center $(x_c, y_c) = (w/2 = 1408, h/2 = 770)$, as shown in figure 3.

Having these values of all the data set images, we obtained the four histograms illustrated in figure 4. Here, the line series correspond to the approximated
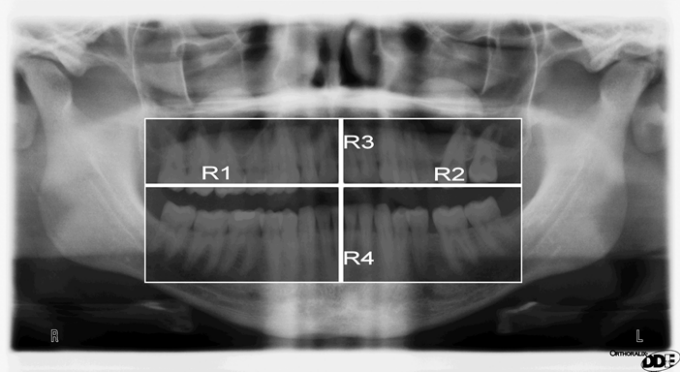
Figure 3: Four lengths extracted of our images database.

normal distribution obtained by a line fitting procedure, defined by the $(\mu,\ \sigma)$ parameters.
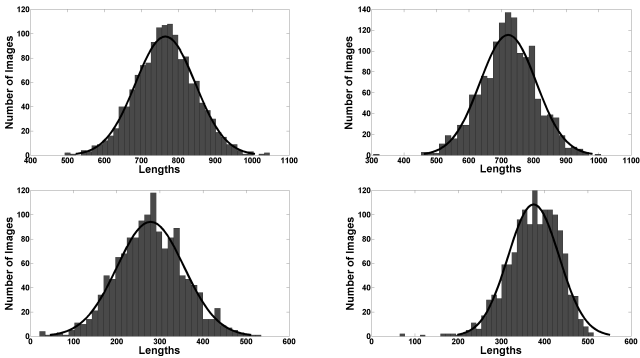

Figure 4: Histogram of the R_i values.

Based on this distribution we can approximate the minimum value for each R_i thereby appropriately cropping the images with a 95% certainty. Furthermore, a defined margin guarantees that slightly different images will be appropriately cropped, even if a small increment of non-useful regions is included. The values obtained were $R_1 \approx 897.77$, $R2 \approx 863.36$, $R3 \approx 406.31$, and $R4 \approx 471.27$.

3.2 Jaws Partition

In this stage we separate the upper and the lower jaws, which is done by applying a polynomial fitting process to a set of primitive pixels located between jaws. This set of pixels is based on the horizontal projection, $v(u)$, of the images, given by 1, where $I(x,i)$ denotes the intensity value at line x and column i.

$$v(u) = \sum_{i=0}^{w} I(x,i) \qquad (1)$$

The initial point is defined at the right extreme of the image and at the line that has the minimum $v(u)$ value, given by 2, where w is the image width.

$$p_0(x_0, w-1) = \arg\min_x(v(u)) \qquad (2)$$

The remaining set of points p_i are regularly spaced, starting from $p_0 : p_i(x_i, (w-1) - W/21)$, where x_i

is obtained similarly to x_0. To avoid too high vertical distances between consecutive p_i, we added the following constraints 3.

$$p_i(x_i, y_i) = \begin{cases} p_i(x_{i+1} + T, y_i), \\ \quad \mid p_i(x_i, y_i) - p_{i+1}(x_{i+1}, y_{i+1}) \mid > T \\ p_i(x_i, y_i),\ otherwise \end{cases}$$
$$(3)$$

Empirically T is the threshold defined by us to avoid the high vertical distances, with the value of $T = 20$. We observed that this step plays a major role in dealing with missing teeth. This method is based on several proposals to perform the separation of jaws ((Chen and Jain 2004) (Jain and Chen 2004) (Shah, Abaza, Ross, and Ammar 2006)). Having the set of $p_i(x_i, y_i)$ primitive points, the division of the jaws is given by the 10th order polynomial, given by $p(x) = a_0 + \ldots + a_{10}x^{10}$, obtained by the least squares fitting algorithm, based on the Vandermond matrix (Dyer and He 2001). This technique is able to achieve impressive accuracy on the data set images, as illustrated in figure 5 and summarized in table 1.
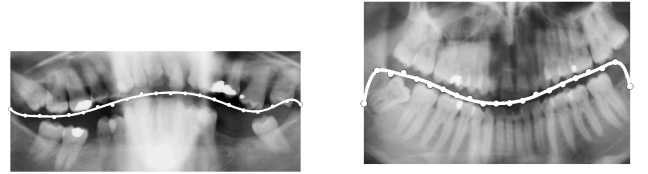

Figure 5: Results of the polynomial fitting by the least squares.

3.3 Teeth Detection

Having both jaws divided, our next goal was to localize the regions corresponding to each teeth, which was based in the detection of the gap of intensities between them. This stage can itself be divided into three sub-stages: For each pixel x between 0 and $w-1$, where w is the image width, we obtain the equation of the perpendicular line to $r(x)$ at the point $(x,\ r(x))$. Then, the average intensity a of the pixels that fall in that line is obtained. Due to the image proprieties, the shape of the teeth and the shape of the polynomial, we found convenient to vary the angle between the line and the polynomial in the $[-15°; +15°]$ interval. Later, for each x we selected the line that minimizes the average intensities a, obtaining a set of $\{a_1,\ \ldots, a_x\}$ values, which is illustrated in figure 5. The key insight is that the a_i values with lowest values should correspond to the partition between consecutive teeth. In order to compensate for abrupt variations in the values we smoothed these values through the use of a Gaussian kernel. Later, we extracted the local minimums of the smoothed signal, hoping that they correspond to the desired partitions. However, we observed that generally the number of local minimums

is higher than the gap valleys (false positives), but the key false negatives are almost inexistent and, for this reason, the subsequent use of an expert-system based approach will easily perform the detection / partition of each tooth. Based on the counting of the detected teeth, the final step crops the upper and lower jaw images into three regions. The left side is composed by three molars and two pre-molars, the front side contains the incisors and a canine and, finally, the right side has three molars and two pre-molars. As reported in section 2, the data set contains many different dentition shapes and number of teeth per images, which led us to crop the images based on two rules. In the first rule, let S_M and S_{PM} the average size of the molar and premolar, respectively, we define a cut limit given by $L_{cut} = 3 * S_M + 2 * S_{PM}$, where L_{cut} corresponds to the maximum crop limit allowed. In the lower jaw it is similar, but in such case the teeth that matter are the inferior. Finally, the second rule measures the existence of five teeth partition lines after the imposed limit L_{cut}. If there are five lines with large differences between the middle point of each line, we suppose that all teeth exist and that the last division line gives the crop coordinates. Figure 6 gives the interval for the average size of the teeth in 1000 sample size, with a 95% certainty.
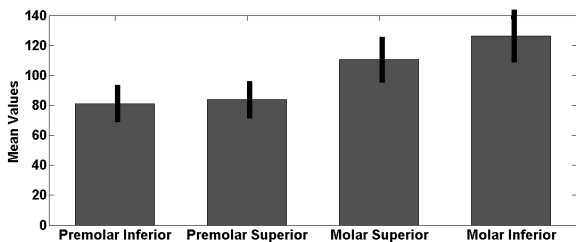

Figure 6: Confidence level for the average size of each type of teeth.

4 Results

In this section we illustrate the results of the above described method that were obtained by visual inspection as showed in table 1. The evaluation of our method is based on a completely independent data sets. It should be stressed that all the results were obtained through 2-folder cross validation. In figure 7

Stages	Stage 1	Stage 2	Stage 3
Results (% of correct)	95.7	92.6	74.6

Table 1: Results of our method for the test data set.

is illustrated one example of our results for the above described method. The results for stage 1 and stage 2 are very optimistic. For the stage 3 the result showed that improvements must be consider, due to the presence of multiple lines for the same gap valley, and in other cases the absence of lines.
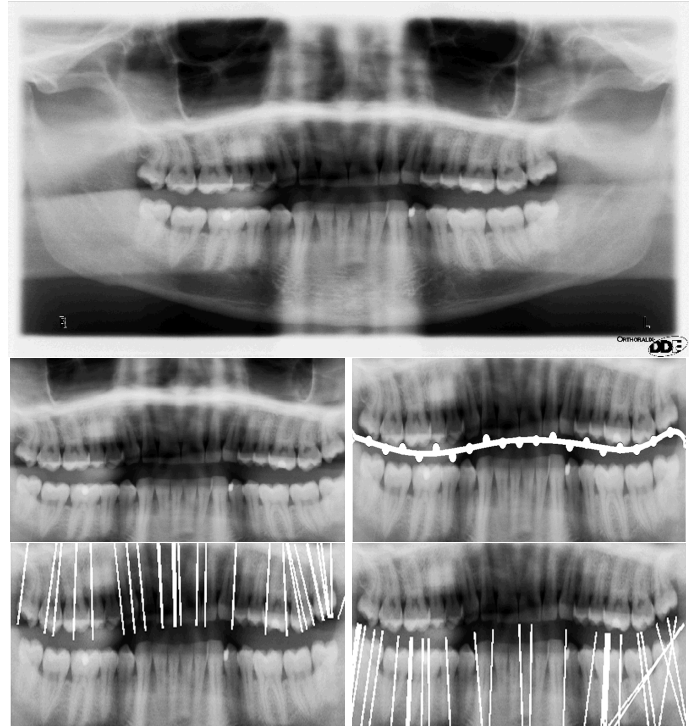

Figure 7: Example of our method results.

5 Conclusions / Future Work

In this paper it is announced the availability of a new data set of panoramic dental X-ray images, which can constitute a tool for the research community in the development of the stomatologic-related applications. This data set has varying morphologic properties that make it more valuable to the scientific community. These varying proprieties include the number of teeth per image, the shape of the mouth and teeth as well as the levels of noise. Also, we gave a method to approximate the panoramic dental X-ray images into bitewing dental X-ray images, which is the type of stomatologic images generally used in image processing methods. This method starts by the definition of a region of interest, followed by the partition of the data into both jaws (through a least squares polynomial fitting process) and, finally, the detection of the teeth in each image which are subsequently counted in order to make the partition into the final desired types of images. As future work our main goal is to start the detection of dental diseases, using the described dental X-ray data set. We plan to start by the detection of dental cavities and move to other types of problems. For that we must improve the accuracy of the teeth segmentation.

REFERENCES

Chen, H. and A. Jain (2004, August). Tooth contour extraction for matching dental radiographs. *Proc. 17th Int'l Conf. Pattern Recognition III*, 522–525.

Dyer, S. and X. He (2001, December). Least-squares fitting of data by polynomials. *IEEE Instrumentation and Measurement Magazine 3*(2), 46–51.

Jain, A., H. Chen, and S. Minut (2003). Dental biometrics: Human identification using dental radiographs. *AVBPA, UK*, 429–437.

Jain, A. K. and H. Chen (2004). Matching of dental x-ray images for human identification. *Pattern Recognition 37*, 1519–1532.

Jain, A. K., L. Hong, and S. Pankanti (2000, February). Biometrics: promising frontiers for emerging identification market. *in Comm. ACM*, 9 1–98.

Li, S., T. Fevens, A. Krzyzak, C. Jin, and S. Li (2007). Semi-automatic computer aided lesion detection in dental x-rays using variational level set. *Pattern Recognition 40*, 2861–2873.

Li, S., T. Fevens, A. Krzyzak, and S. Li (2006). An automatic variational level set segmentation framework for computer aided dental x-rays analysis in clinical environments. *Computerized Medical Imaging and Graphics 30*, 65–74.

Lin, J., K. Cheng, and C. Mao (1996, August). A fuzzy hopfield neural network for medical image segmentation. *IEEE Trans. Nucl. Sci. 43*(4), 2389–2398.

Nomir, O. and M. Abdel-Mottaleb (2005). A system for human identification from x-ray dental radiographs. *Pattern Recognition 38*, 1295–1305.

Nomir, O. and M. Abdel-Mottaleb (2007). Human identification from dental x-ray images based on the shape and appearance of the teeth. *IEEE Transactions on Information Forensics and Security 2*(2).

Nomir, O. and M. Abdel-Mottaleb (2008, June). Fusion of matching algorithms for human identification using dental x-ray radiographs. *IEEE Transactions on Information Forensics and Security 3*(2).

Said, E. H., D. E. M. Nassar, G. Fahmy, and H. H. Ammar (2006, June). Teeth segmentation in digitized dental x-ray films using mathematical morphology. *IEEE Transactions on Information Forensics and Security*.

Shah, S., A. Abaza, A. Ross, and H. Ammar (2006, June). Automatic tooth segmentation using active contour without edges. *IEEE Biometrics Symposium 1*(2).

Shiffman, S., G. D. Rubin, and S. Naple (2000, November). Semi-automatic computer aided lesion detection in dental x-rays using variational level set. *IEEE Trans. Med. Imag. 19*(11), 1064–1074.

Zhou, J. and M. Abdel-Mottaleb (2005). A content-based system for human identification based on bitewing dental x-ray images. *Pattern Recognition 38*, 2132–2142.